Research Square

Preprints are preliminary reports that have not undergone peer review.
They should not be considered conclusive, used to inform clinical practice,
or referenced by the media as validated information.

Artificial Hibernation as a Novel Metabolic Therapy for Suppressing Melanoma Growth and Metastasis

Amirhosein Kefayat

ahkefayat@yahoo.com

University of Edinburgh Western General Hospital: Western General Hospital https://orcid.org/0000-0002-0616-8870

Niyousha Vakilzadehian

King's College Hospital NHS Foundation Trust

Mahshid Bahrami

University of Sussex

Mojtaba Karami

Tehran University: University of Tehran

Fatemeh Ghahremani

Arak University of Medical Sciences https://orcid.org/0000-0002-7244-6066

Research Article

Keywords: Artificial hibernation, Hypometabolism, Cancer, Metastasis, Tumor metabolism

Posted Date: July 23rd, 2026

DOI: https://doi.org/10.21203/rs.3.rs-10046575/v1

License: This work is licensed under a Creative Commons Attribution 4.0 International License.
Read Full License

Abstract

Background:

Melanoma is a highly aggressive malignancy characterized by rapid progression, early metastasis, and resistance to therapy. Given its high metabolic demand, targeting systemic tumor metabolism may represent a novel therapeutic strategy.

Methods:

Artificial hibernation was induced in C57BL/6 mice bearing B16-F10 melanoma tumors using intraperitoneal administration of 5'-adenosine monophosphate (AMP). Tumor growth, metastatic burden, and metabolic activity were evaluated using histopathology and ^{18}F-FDG PET imaging.

Results:

Artificial hibernation induced a reversible hypometabolic state and significantly inhibited tumor growth. By day 28 after cancer cells implantation, mean tumor volume was reduced from 1920.3 ± 289.1 mm³ in controls to 706.2 ± 76.88 mm³ in hibernated mice (~ 63.2%), while tumor weight decreased from 4.4 ± 0.69 g to 1.2 ± 0.3 g (~ 72.7%). Metastatic burden was also markedly suppressed, with lung metastatic nodules reduced from 15.5 ± 6.1 to 6.2 ± 1.5 (~ 60.0%) and lung weight decreased from 1.03 ± 0.20 g to 0.30 ± 0.01 g (~ 70.9%) 20 days after intravenous injection of cancer cells. FDG-PET imaging demonstrated global metabolic suppression, with tumor glucose uptake reduced from 2.65 ± 0.49 to 1.53 ± 0.34 (~ 42%) and skeletal muscle uptake reduced by ~ 63%. Importantly, FDG uptake within metastatic lung lesions was also significantly reduced (~ 50%), indicating pronounced metabolic suppression within metastatic colonies. Notably, metabolic suppression was maintained across different tumor sizes, indicating efficacy in both moderate and large tumors.

Conclusion:

Artificial hibernation significantly suppresses melanoma growth and metastasis through systemic metabolic modulation. These findings support hypometabolic therapy as a novel and potentially translatable strategy for the treatment of aggressive and advanced cancers.

1. Introduction

Melanoma is among the most aggressive and lethal forms of cancer, characterized by rapid progression, early dissemination, and a high propensity for metastasis. Despite advances in targeted therapies and immunotherapy, a substantial proportion of patients develop resistance to treatment, leading to disease progression and poor clinical outcomes [1]. Metastatic melanoma, in particular, remains associated with

significant mortality, as the spread of tumor cells to distant organs dramatically limits the effectiveness of current therapeutic strategies. These challenges highlight the urgent need for innovative treatment approaches that can effectively target both primary tumor growth and metastatic dissemination [2].

A defining feature of melanoma, as with many malignancies, is its high metabolic demand. Cancer cells rely on continuous energy production to sustain rapid proliferation, survival, and metastatic activity. This metabolic dependency creates a potential vulnerability that can be therapeutically exploited. However, most current treatments focus on molecular signaling pathways or immune modulation, with relatively limited attention given to targeting systemic metabolic processes [3, 4]. Developing strategies that disrupt tumor energetics at a systemic level may therefore provide a novel and complementary approach to cancer therapy.

Hibernation is a natural physiological state observed in certain mammals, characterized by a reversible and tightly regulated suppression of metabolic activity. During hibernation, organisms significantly reduce their core body temperature, oxygen consumption, and overall energy expenditure, enabling survival under extreme environmental conditions. Importantly, this hypometabolic state is not associated with tissue damage and can be rapidly reversed upon return to normal conditions [5, 6]. Recent studies have demonstrated that hibernation-like states can be pharmacologically induced in non-hibernating species using agents such as 5'-adenosine monophosphate (AMP), which acts centrally to lower the thermoregulatory set point and suppress metabolic activity [7, 8].

The induction of a systemic hypometabolic state presents a unique opportunity to target the metabolic vulnerabilities of cancer. While normal tissues can adapt to reduced energy availability by entering a reversible quiescent state, cancer cells, due to their high metabolic demands, may be less capable of such adaptation. This imbalance suggests that systemic metabolic suppression could selectively impair tumor growth and progression while preserving normal tissue function [8]. Moreover, metastasis is an energetically intensive process requiring sustained cellular migration, invasion, and colonization, making it particularly susceptible to metabolic disruption [9].

In the present study, according to the best of our knowledge for the first time, we aim to validate artificial hibernation as a novel and potentially translatable therapeutic approach that targets cancer through systemic metabolic modulation to prevent tumor growth and metastasis. We investigated the effects of AMP-induced artificial hibernation in a B16-F10 murine melanoma model, a well-established melanoma model known for its rapid growth and strong metastatic potential. We evaluated the impact of induced hypometabolism on tumor growth, metastatic spread, and systemic metabolic activity using a combination of in vivo tumor analysis, histopathology, and FDG-PET imaging.

2. Materials and Methods

2.1. Animal Ethics

All animal experiments were conducted in accordance with the ARRIVE guidelines and complied with the European Communities Council Directive (2010/63/EU) as well as institutional standards for the care and use of laboratory animals. All procedures were approved by the Ethics Committee of Arak University of Medical Sciences (IR.ARAKMU.REC.1400.092).

2.2. Induction of Artificial Hibernation

Artificial hibernation was induced using 5'-adenosine monophosphate (AMP) based on previously established protocols [10]. Briefly, AMP (0.5 mg/g body weight), dissolved in phosphate-buffered saline (PBS), was administered via intraperitoneal injection. Following injection, animals were maintained at an ambient temperature of 25°C. Mice that did not exhibit a hypometabolic response were excluded from the study. Core body temperature (Tc) was measured hourly for 8 hours using a rectal probe (RET-3, Braintree Scientific, USA). Surface temperature (Ts) was monitored using a thermal imaging camera. General physiological status was assessed by clinical observation and thermal imaging. Locomotor activity during the hibernation state was assessed using 20-minute video recordings. Movement was quantified using a custom Python-based algorithm by calculating frame-to-frame differences to generate a movement index. Blood glucose levels were measured 6 hours after AMP injection via cardiac puncture using a glucometer.

2.3. Cell Culture

Murine melanoma (B16-F10) cell lines were obtained from the Pasteur Institute (Tehran, Iran). B16-F10 cells were cultured in Dulbecco's Modified Eagle's Medium (DMEM) (Sigma-Aldrich, USA). Media were supplemented with 10% fetal bovine serum (FBS; Gibco, USA) and 1% penicillin–streptomycin. Cells were incubated at 37°C in a humidified atmosphere containing 5% CO_2.

2.4. Tumor implantation and Treatment Protocol

Female C57BL/6 mice (20–25 g) were housed under standard laboratory conditions (24 ± 2°C, 50 ± 10% humidity, 12-hour light/dark cycle) with ad libitum access to food and water. After a 7-day acclimatization period, mice were subcutaneously injected in the right flank with 2×10^6 B16-F10 cells suspended in 50 µL of DMEM-F12 (Sigma, USA). Once tumors became palpable, mice were randomly assigned to two groups (n = 5 per group) including Control group which received intraperitoneal PBS and Hibernation group which received AMP (0.5 mg/g, intraperitoneally) daily for 20 days to induce 4–5 hours of artificial hibernation every day. Tumor dimensions were measured every three days using a digital caliper. Tumor volume was calculated as:

Tumor volume = (length × width²) / 2

Body weight was recorded at the same time points.

2.5. Metastasis Assessment and Histopathology

To establish a metastatic model, mice were intravenously injected with 1×10^6 B16-F10 cells. Animals were randomly divided into control and hibernation groups (n = 5 per group) and treated as described

above. After 20 days, mice were euthanized, and lungs and liver were harvested, weighed, and fixed in 10% neutral buffered formalin. Tissue samples were processed, embedded in paraffin, and sectioned into 4 μm slices. Sections were stained with hematoxylin and eosin (H&E). Metastatic burden was evaluated by counting the number of metastatic nodules and examining at least 10 randomly selected microscopic fields per sample under a 10× objective lens. Whole lung sections were also analyzed to determine total metastatic involvement.

2.6. Small-Animal PET Imaging

Small-animal PET imaging was performed using a micro-PET scanner (Xtrim PET). Mice were anesthetized and injected intravenously with approximately 100 μCi of ^{18}F-FDG. Three-dimensional regions of interest (ROIs) were manually defined on whole-body coronal images. Glucose uptake was expressed as activity uptake ratio using the following formula:

$$100 \times (\text{ROI counts}) / (\text{total body counts} - \text{ROI counts})$$

Tumor, muscle, brain, and brown adipose tissue (BAT) uptake were quantified for metabolic analysis.

2.7. Statistical Analysis

Data are presented as mean ± standard deviation (SD). Statistical comparisons between groups were performed using an unpaired Student's t-test (JMP 14.0, SAS Institute). A p-value < 0.05 was considered statistically significant. Survival data were analyzed using Kaplan–Meier curves, and differences between groups were evaluated using the log-rank test.

3. Results

3.1 Induction of artificial hibernation in the C56BL6 mice

Artificial hibernation was successfully induced in C57BL/6 mice following intraperitoneal administration of AMP (0.5 mg/g body weight). Within approximately 30 minutes post-injection, animals exhibited a marked and progressive decline in core body temperature, reaching a nadir of ~30 °C under ambient conditions (25 °C). This hypometabolic state was accompanied by near-complete suppression of voluntary movement, with only occasional minimal involuntary activity observed (Figure 1A), confirming effective induction of a hibernation-like phenotype.

Thermal imaging analysis further demonstrated a rapid and sustained reduction in surface body temperature following AMP administration (Figure 1B). Quantitative assessment revealed that both head and tumor surface temperatures in the hibernation group decreased significantly compared to control animals, beginning as early as 30-60 minutes post-injection and reaching their lowest levels between 120–240 minutes (Figure 1C). During this period, hibernated mice maintained a stable hypothermic

plateau for approximately 3 hours, after which body temperature gradually returned to baseline within 60 minutes, indicating a reversible and controlled hypometabolic state.

Importantly, differential thermal behavior between tumor and normal tissues was observed (Figure 1B & C). In control non-hibernated tumor-bearing mice, tumor regions consistently exhibited higher surface temperatures (approximately 1–2 °C above adjacent tissues), likely reflecting increased metabolic activity and enhanced perfusion characteristic of rapidly proliferating tumors. In contrast, induction of artificial hibernation led to a notable inversion of this pattern. Tumor regions in hibernated mice displayed a more pronounced reduction in surface temperature compared to surrounding tissues, becoming relatively cooler by approximately 1–2 °C. This tumor-specific thermal response suggests a heightened sensitivity of malignant tissue to systemic metabolic suppression. The exaggerated cooling effect in tumors may reflect impaired metabolic adaptability, reduced perfusion, or altered microvascular regulation under hypometabolic conditions. These findings indicate that artificial hibernation not only induces global physiological suppression but may also selectively impact tumor metabolism, potentially exposing a vulnerability that could be therapeutically exploited. Overall, these results confirm the successful establishment of a reversible artificial hibernation model and demonstrate a distinct and preferential thermal response of tumor tissue to induced hypometabolism.

3.2. Effect of Artificial Hibernation Induction on Melanoma Tumor Growth

In this study, we utilized the B16-F10 murine melanoma model in C57BL/6 mice, a highly aggressive and rapidly growing tumor model [7]. As shown in Figure 2A, tumors became palpable within a few days following subcutaneous implantation. At the 10^{th} day after cancer cells implantation, the tumor-bearing mice were randomly divided into two groups. Before the initiation of treatment, there was no significant difference ($P > 0.05$) in mean tumor volume between the control and hibernation groups, confirming appropriate randomization. Daily induction of artificial hibernation via intraperitoneal AMP injection resulted in a significant suppression of tumor growth. Tumor volume increased progressively in both groups; however, the rate of growth was markedly reduced in the hibernation group. By day 28, the mean tumor volume in the control group reached 1920.3 ± 289.1 mm^3, whereas it was significantly lower in the hibernation group (706.2 ± 76.88 mm^3), corresponding to an approximate 63.2% reduction in tumor volume compared to controls ($P < 0.05$) (Figure 2A).

Monitoring of tumor-bearing mice body weight (Figure 2B) further supported these findings. Mice in the control group exhibited a greater increase in body weight over time compared to the hibernation group, indicating a higher tumor burden, whereas the reduced weight gain in the hibernation group is consistent with suppressed tumor progression.

Representative images of harvested tumors (Figure 2C) visually confirm the significant difference in tumor size between groups, with markedly smaller tumors observed in the hibernation-treated mice. Quantitative analysis of tumor weight at day 28 (Figure 2D) demonstrated that the mean tumor weight in the hibernation group (1.2 ± 0.3 g) was significantly lower than in the control group (4.4 ± 0.69 g), corresponding to an approximate 72.7% reduction in tumor mass ($P < 0.05$). Overall, these data indicate

that repeated induction of artificial hibernation significantly inhibits melanoma tumor growth, both in terms of tumor volume progression and final tumor burden.

3.2 Artificial Hibernation Induces Systemic Metabolic Suppression and Reduces Tumor Glucose Uptake

To investigate the metabolic effects of artificial hibernation, whole-body glucose utilization was assessed using ^{18}F-FDG PET imaging in tumor-bearing mice. Representative PET images (Figure 3A–B, Figure S1) demonstrate a pronounced reduction in global metabolic activity in artificially hibernated tumor-bearing mice compared to controls. Under control (non-hibernated) conditions, high FDG uptake was observed in multiple tissues, including tumor, muscle, and brain. In contrast, during artificial hibernation, a marked suppression of whole-body FDG uptake was evident, indicating a systemic hypometabolic state.

In accordance with this whole-body metabolic suppression, residual FDG uptake significantly decreased within the tumor region (dashed circles), although substantially tumor tissue showed a bit more resistance to decrease its metabolic activity compared to other body parts. Quantitative analysis confirmed that tumor metabolic activity, expressed as tumor-to-background ratio (TBR), was decreased about 34.5% in the hibernation group (Figure 3C), indicating a significant reduction in tumor glucose uptake.

Systemic metabolic suppression was further supported by a marked, about 46%, decrease in skeletal muscle glucose uptake (% of injected FDG dose uptake) in hibernated animals compared to non-hibernated controls (Figure 3D), reflecting reduced peripheral energy demand. Interestingly, analysis of brain metabolism revealed relative preservation of glucose uptake, as indicated by maintained brain-to-background ratio (BBR) (Figure 3E), suggesting preferential protection of essential organ function during the hypometabolic state. In addition, brown adipose tissue (BAT) activity was increased in hibernated mice (Figure 3F), likely reflecting thermogenic adaptation and metabolic regulation during artificial hibernation.

Overall, these findings demonstrate that artificial hibernation induces a profound metabolic reprogramming characterized by global suppression of glucose utilization, reduced tumor metabolic activity, preservation of brain metabolism, and activation of BAT. Although tumor showed significant decrease in its metabolism, they still were more active during hibernation compared with other body regions like muscles. This systemic metabolic shift may underlie the observed anti-tumor and anti-metastatic effects of artificial hibernation.

3.3. Effect of Artificial Hibernation on Melanoma Metastasis

To evaluate the effect of artificial hibernation on metastatic progression, a diffuse melanoma metastasis model was established by intravenous injection of 1×10^6 B16-F10 cells into C57BL/6 mice. Following tumor cell inoculation, animals underwent daily induction of artificial hibernation using AMP. After 20 days, lungs and livers were harvested for macroscopic, metabolic, and histopathological analyses.

Macroscopic examination of the lungs (Figure 3A) revealed extensive metastatic involvement in control mice, characterized by numerous large and densely distributed melanoma nodules. In contrast, lungs from hibernation-treated animals exhibited markedly fewer and smaller metastatic lesions, indicating a substantial suppression of metastatic colonization. Quantitative analysis confirmed these observations (Figure 3B), showing that the mean number of metastatic lung nodules decreased from 15.5 ± 6.1 in the control group to 6.2 ± 1.5 in the hibernation group, corresponding to an approximate 60.0% reduction in metastatic burden ($P < 0.05$). Consistently, lung weight (Figure 3C), reflecting the overall extent of tumor infiltration, was significantly reduced in the hibernation group (0.30 ± 0.01 g) compared to controls (1.03 ± 0.20 g), representing an approximate 70.9% reduction in metastatic tumor load ($P < 0.05$).

To further assess the metabolic activity of metastatic lesions, ^{18}F-FDG PET imaging was performed in mice bearing lung metastases (Figure 3D). A pronounced reduction in FDG uptake was observed in the lung regions of hibernated animals compared to controls, indicating significant suppression of metabolic activity within metastatic colonies. Notably, this reduction appeared even more prominent than that observed in primary tumors, suggesting that metastatic lesions may be particularly sensitive to systemic hypometabolic conditions.

Histopathological evaluation (Figure 3E) supported these findings, demonstrating extensive metastatic infiltration and disruption of normal alveolar architecture in control mice. In contrast, lungs from the hibernation group showed markedly fewer metastatic foci and preservation of normal tissue structure. Analysis of liver tissues revealed only occasional small metastatic foci in control animals, whereas no detectable metastasis was observed in the hibernation-treated group. This finding suggests that artificial hibernation may effectively inhibit secondary metastatic dissemination to distant organs.

Overall, these results demonstrate that artificial hibernation significantly suppresses melanoma metastasis at both structural and metabolic levels, reducing metastatic burden, decreasing metabolic activity of metastatic lesions, and preserving organ architecture.

3.4. Effect of Tumor Size on Metabolic Response to Artificial Hibernation

To determine whether tumor size influences the metabolic response to artificial hibernation, ^{18}F-FDG PET imaging was performed in mice bearing tumors of different sizes. As shown in Figure 4 and Figure S1, tumor metabolic activity, expressed as tumor-to-background ratio (TBR), was lower in larger tumors (14 days post-implantation, 1.13 ± 0.13) compared to smaller tumors (28 day post-implantation, 1.64 ± 0.25), corresponding to an approximate 31% reduction. However, this difference did not reach statistical significance ($P = 0.10$). These findings suggest that although larger tumors may exhibit reduced baseline metabolic activity, the overall metabolic response to artificial hibernation is not significantly dependent on tumor size. Importantly, this indicates that the hypometabolic effects of artificial hibernation are maintained across different tumor burdens, supporting its potential applicability in both early- and advanced-stage disease.

4. Discussion

In the present study, we demonstrate that induction of artificial hibernation via AMP leads to significant suppression of melanoma tumor growth and, more importantly, a marked inhibition of metastatic progression. Using the highly aggressive B16-F10 melanoma model, our findings provide the first evidence that artificial hibernation can be effectively applied as a therapeutic strategy in metastatic melanoma, a cancer characterized by rapid dissemination, treatment resistance, and high mortality [1].

Metastasis remains the primary cause of melanoma-related death, and metastasis is particularly dependent on energy-intensive processes such as invasion, circulation, and colonization of distant organs [2, 9]. Our data demonstrate that artificial hibernation significantly reduces metastatic burden, as evidenced by a substantial decrease in lung nodules and tumor mass. Importantly, FDG-PET imaging revealed a pronounced reduction in metabolic activity within metastatic lesions, which appeared even more sensitive to hypometabolic conditions than primary tumors. This observation suggests that metastatic cells may have limited metabolic adaptability and are therefore particularly vulnerable to systemic energy restriction.

The PET findings further support the mechanistic basis of this approach. Artificial hibernation induced a global suppression of glucose metabolism, with a marked decrease in skeletal muscle uptake and a significant reduction in tumor metabolic activity. Despite this, residual tumor uptake persisted, indicating that cancer cells retain partial metabolic function; however, this level appears insufficient to sustain proliferation and metastatic expansion. The relative preservation of brain metabolism highlights the controlled and physiological nature of this hypometabolic state, distinguishing it from pathological metabolic collapse [11].

An important aspect of this study is the use of AMP as the hibernation-inducing agent. Among available methods, AMP offers a significant advantage due to its endogenous nature and favorable safety profile. In contrast to agents such as hydrogen sulfide (H_2S), which induce hypometabolism through direct inhibition of mitochondrial respiration and are associated with toxicity and narrow therapeutic windows [12], AMP acts through centrally regulated mechanisms, primarily via adenosine receptor-mediated modulation of thermoregulation [13]. This allows for a reversible and controlled induction of hypometabolism without direct mitochondrial toxicity. In our study, repeated induction of artificial hibernation did not result in detectable tissue damage, supporting the translational potential of AMP-based approaches.

Another key finding is that the metabolic response to artificial hibernation was not significantly affected by tumor size. Although larger tumors exhibited lower baseline metabolic activity, the relative suppression induced by hibernation remained consistent across tumor burdens. This suggests that artificial hibernation may be effective even in large or advanced tumors, including those that are clinically unresectable or resistant to conventional therapies. In this context, systemic metabolic suppression may represent a complementary therapeutic strategy where current treatment options are limited.

These findings are consistent with our previous work in a murine breast cancer model, where artificial hibernation similarly inhibited tumor growth and metastasis. The present study was designed to validate

this concept in a biologically distinct and more aggressive cancer type. The comparable efficacy observed across models suggests that artificial hibernation targets a fundamental vulnerability in cancer biology, its dependence on sustained energy supply, rather than tumor-specific signaling pathways.

This study has some limitations. While our results clearly demonstrate the anti-tumor and anti-metastatic effects of artificial hibernation at physiological and metabolic levels, the precise molecular mechanisms underlying these effects were not fully elucidated. Further investigations are required to characterize the cellular pathways involved, including potential alterations in tumor metabolism, microenvironment, angiogenesis, and immune responses. These aspects are currently under active investigation by our group. Importantly, the primary objective of this study was to establish proof-of-concept that artificially induced hibernation can function as a therapeutic strategy against cancer and metastasis.

5. Conclusion

In conclusion, this study demonstrates that induction of artificial hibernation via AMP effectively suppresses melanoma tumor growth and significantly reduces metastatic dissemination. These anti-tumor effects are mediated through systemic metabolic suppression, highlighting a fundamentally different therapeutic approach. Importantly, artificial hibernation was effective across different tumor burdens and showed pronounced inhibitory effects on metastasis, suggesting particular relevance for advanced and unresectable disease. By targeting the metabolic dependencies of cancer cells, artificial hibernation exploits a key vulnerability of tumor biology while preserving normal physiological function. The associated reduction in tumor and metastatic metabolic activity, supported by FDG-PET imaging, further confirms the role of controlled hypometabolism in limiting cancer progression. Collectively, these findings establish artificial hibernation as a novel and promising strategy for melanoma treatment and provide a foundation for future studies aimed at clinical translation and combination with existing therapies.

Abbreviations

AMP 5'-adenosine monophosphate

Declarations

Consent for publication

All authors read and confirmed the manuscript for publication

Availability of data and material

Data would be available on reasonable request.

Authors' contributions

A.K. conceived and designed the study, developed the research methodology, conducted the literature review, performed data analysis and interpretation, drafted the original manuscript, and critically revised the manuscript for important intellectual content. A.K. also supervised the overall project and takes primary responsibility for the integrity and accuracy of the work. N.V. contributed to data collection, literature review, data interpretation, manuscript drafting, and revision of the manuscript. M.B. contributed to data collection, data analysis, and manuscript revision. M.K. contributed to data interpretation and critically reviewed the manuscript. F.G. supervised the study, provided scientific guidance, contributed to the interpretation of findings, and critically revised the manuscript for important intellectual content. All authors read and approved the final manuscript.

Acknowledgment

Authors would like to acknowledge Preclinical Lab, Core Facility, Tehran University of Medical Sciences, Tehran, Iran, for providing the in vivo imaging and image processing services for this research.

Funding

This study was funded by Arak University of Medical Sciences (3930). None of the authors have received research grants from any company.

Competing Interest

The authors declare that they have no known competing financial interests or personal relationships that could have appeared to influence the work reported in this paper.

Ethical approval

All animal experiments and procedures were verified according to the guidelines of the Institutional Animal Care and Ethics Committee of Arak University of Medical Sciences. This article does not contain any studies with human participants performed by any of the authors.

References

1. Schadendorf D, et al. Melanoma Lancet. 2018;392(10151):971–84.
2. Steeg PS. Targeting metastasis. Nat Rev Cancer. 2016;16(4):201–18.
3. Pavlova NN, Thompson CB. The emerging hallmarks of cancer metabolism. Cell Metabol. 2016;23(1):27–47.
4. Faubert B, Solmonson A, DeBerardinis RJ. Metabolic reprogramming and cancer progression. Science. 2020;368(6487):eaaw5473.
5. Storey KB, Storey JM. Metabolic rate depression in animals: transcriptional and translational controls. Biol Rev. 2004;79(1):207–33.

6. Carey HV, Andrews MT, Martin SL. Mammalian hibernation: cellular and molecular responses to depressed metabolism and low temperature. Physiol Rev. 2003;83(4):1153–81.
7. Swoap SJ, Rathvon M, Gutilla M. AMP does not induce torpor. Am J Physiology-Regulatory Integr Comp Physiol. 2007;293(1):R468–73.
8. Tao Z, Zhao Z, Lee CC. 5'-Adenosine monophosphate induced hypothermia reduces early stage myocardial ischemia/reperfusion injury in a mouse model. Am J translational Res. 2011;3(4):351.
9. LeBleu VS, et al. PGC-1α mediates mitochondrial biogenesis and oxidative phosphorylation in cancer cells to promote metastasis. Nat Cell Biol. 2014;16(10):992–1003.
10. Zhang J. Constant darkness is a circadian metabolic signal in mammals. Nature. 2006;439:340–3. Lee CC.
11. Kalluri R. The biology and function of fibroblasts in cancer. Nat Rev Cancer. 2016;16(9):582–98.
12. Blackstone E, Morrison M, Roth MB. H2S induces a suspended animation-like state in mice. Science. 2005;308(5721):518–518.
13. Zhang M et al. *Drug-induced hypothermia in stroke models: does it always protect?* CNS & Neurological Disorders-Drug Targets-CNS & Neurological Disorders), 2013. 12(3): pp. 371–380.

Figures

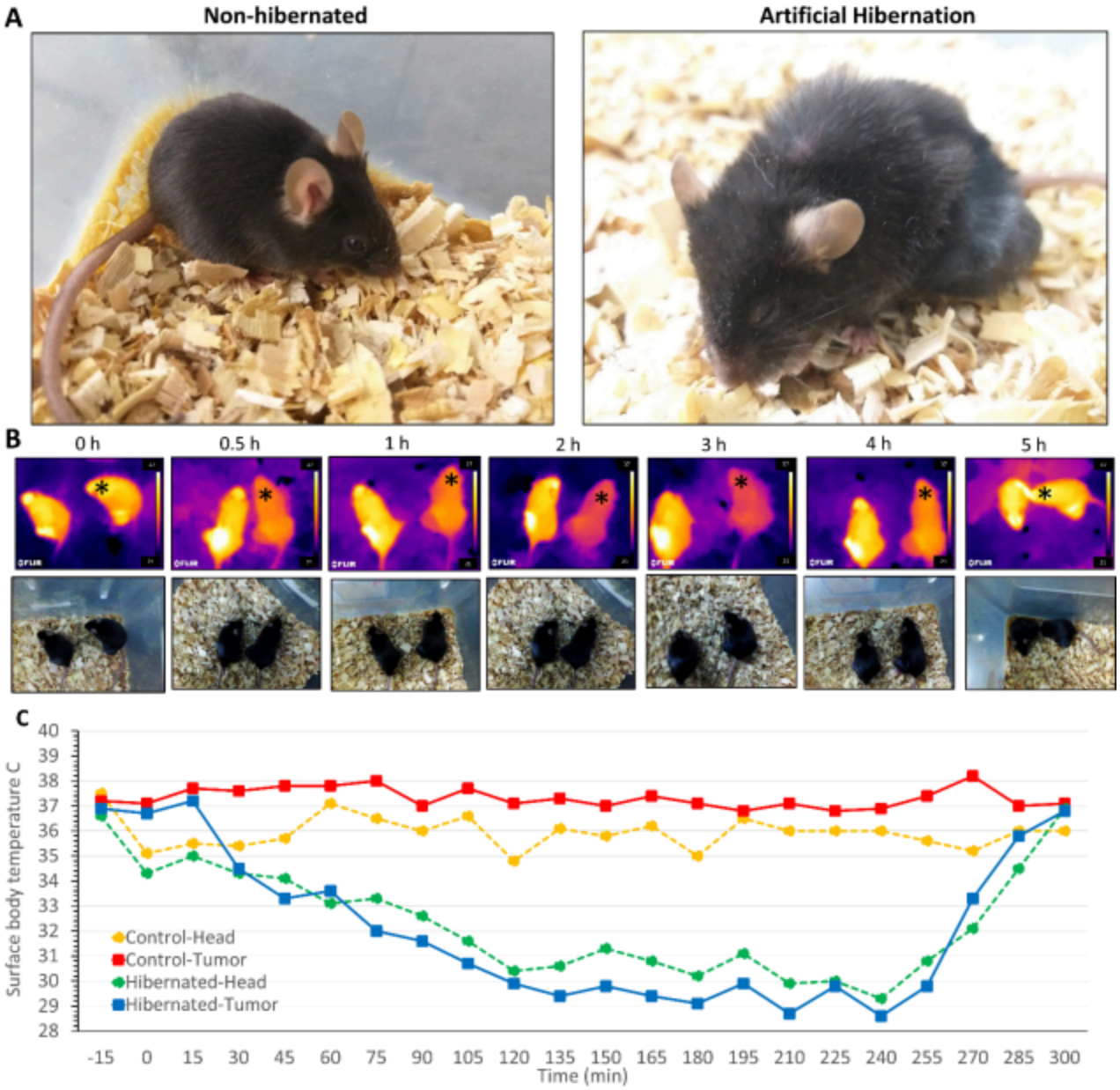


Figure 1

Artificial hibernation induction and its effect on body and tumor temperature. A) Representative images of control (non-hibernated) and AMP-treated (artificially hibernated) C57BL/6 mice, demonstrating reduced activity and a characteristic curled posture during the hypometabolic state. (B) Serial thermal imaging of tumor-bearing mice at 0, 0.5, 1, 2-, 3-, 4-, and 5-hours following AMP administration, illustrating the progressive decline and subsequent recovery of body surface temperature. Asterisks (*) indicate the artificially hibernated mouse. (C) Quantitative analysis of surface temperature measured in the head and tumor regions over time using thermal imaging. In control non-hibernated mice, tumor regions exhibited consistently higher temperatures compared to surrounding tissues, whereas in hibernated mice, a marked reduction in both head and tumor temperatures was observed, with tumor regions showing a relatively greater decrease during the hypometabolic phase. Data represent dynamic temperature changes over the experimental time course.

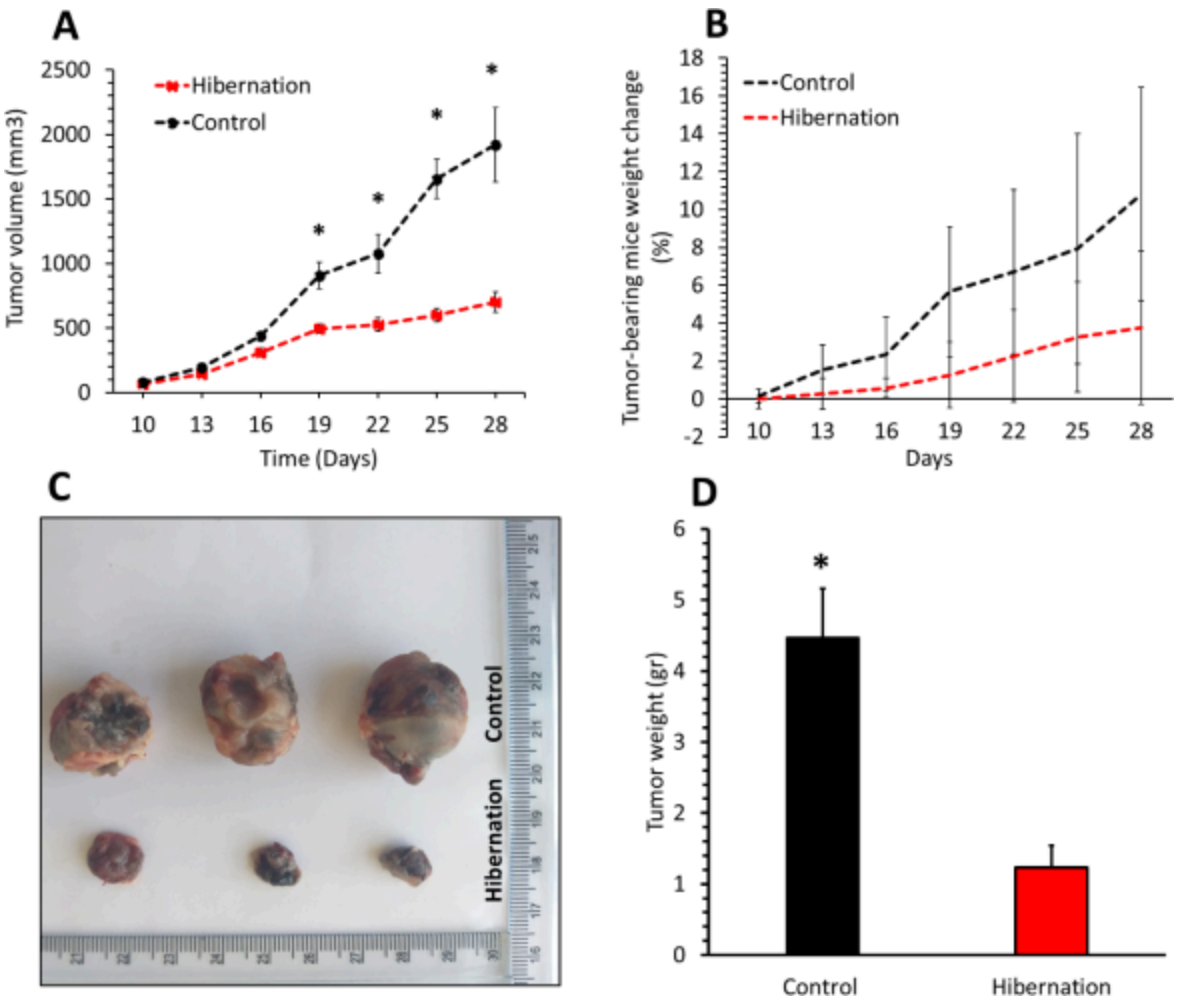


Figure 2

Effect of artificial hibernation on melanoma tumor growth. A) Calculated tumors volume and B) tumor-bearing mice body weight progression monitoring since 10th day after cancer cells implantation. C) Macroscopic appearance of harvested tumors at day 28 after cancer cells implantation in the control and hibernation groups. D) The harvested tumors weight in 28th day after cancer cell implantation. Statistical analysis was performed using unpaired Student's t-test; ns: not significant and *: statistically significant ($P < 0.05$).

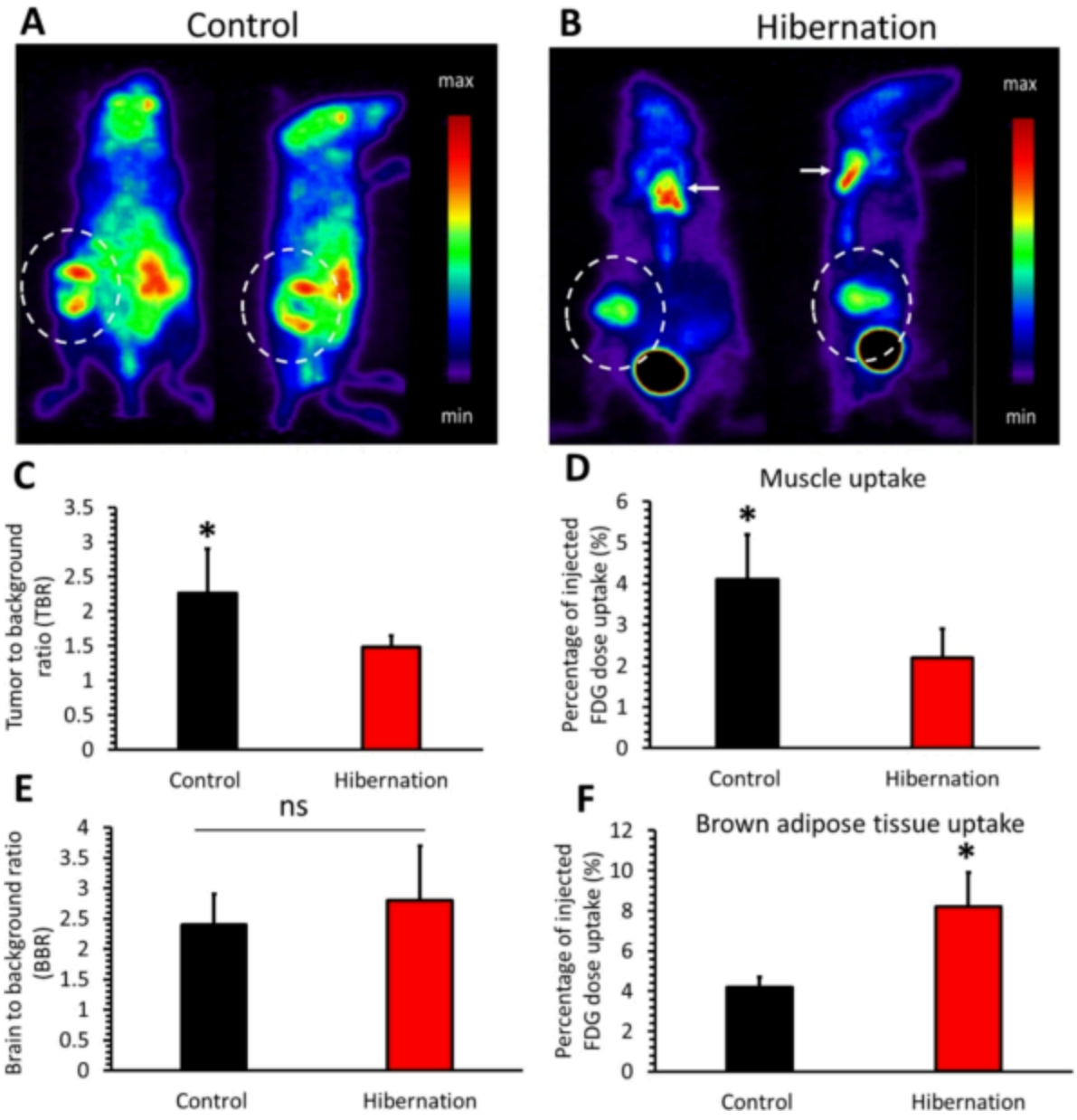


Figure 3

Artificial hibernation induces systemic metabolic suppression and reduces tumor glucose uptake. (A) Representative ^{18}F-FDG PET images of tumor-bearing mice under control (non-hibernated) conditions and (B) during artificial hibernation, shown in sagittal and frontal views. Dashed circles indicate the tumor region and arrow points to the brown adipose tissue region. A marked reduction in whole-body metabolic activity is observed during hibernation, while despite significant decrease in the tumor metabolism activity, tumor uptake remains detectable relative to suppressed background tissues. Please see Figure S1. (C–F) Quantitative analysis of tissue-specific metabolic activity. (C) Tumor metabolic activity, expressed as tumor-to-background ratio (TBR), is reduced in hibernated animals compared to controls. (D) Skeletal muscle glucose uptake (% injected dose) is significantly decreased in the hibernation group, indicating systemic hypometabolism. (E) Brain-to-background ratio (BBR) demonstrates relative preservation of brain glucose metabolism. (F) Brown adipose tissue (BAT) uptake (% injected dose) is increased in the hibernation group, suggesting enhanced thermogenic activity. Data

are presented as mean ± SD. Statistical analysis was performed using an unpaired Student's t-test; ns, not significant; P < 0.05 indicates statistical significance.

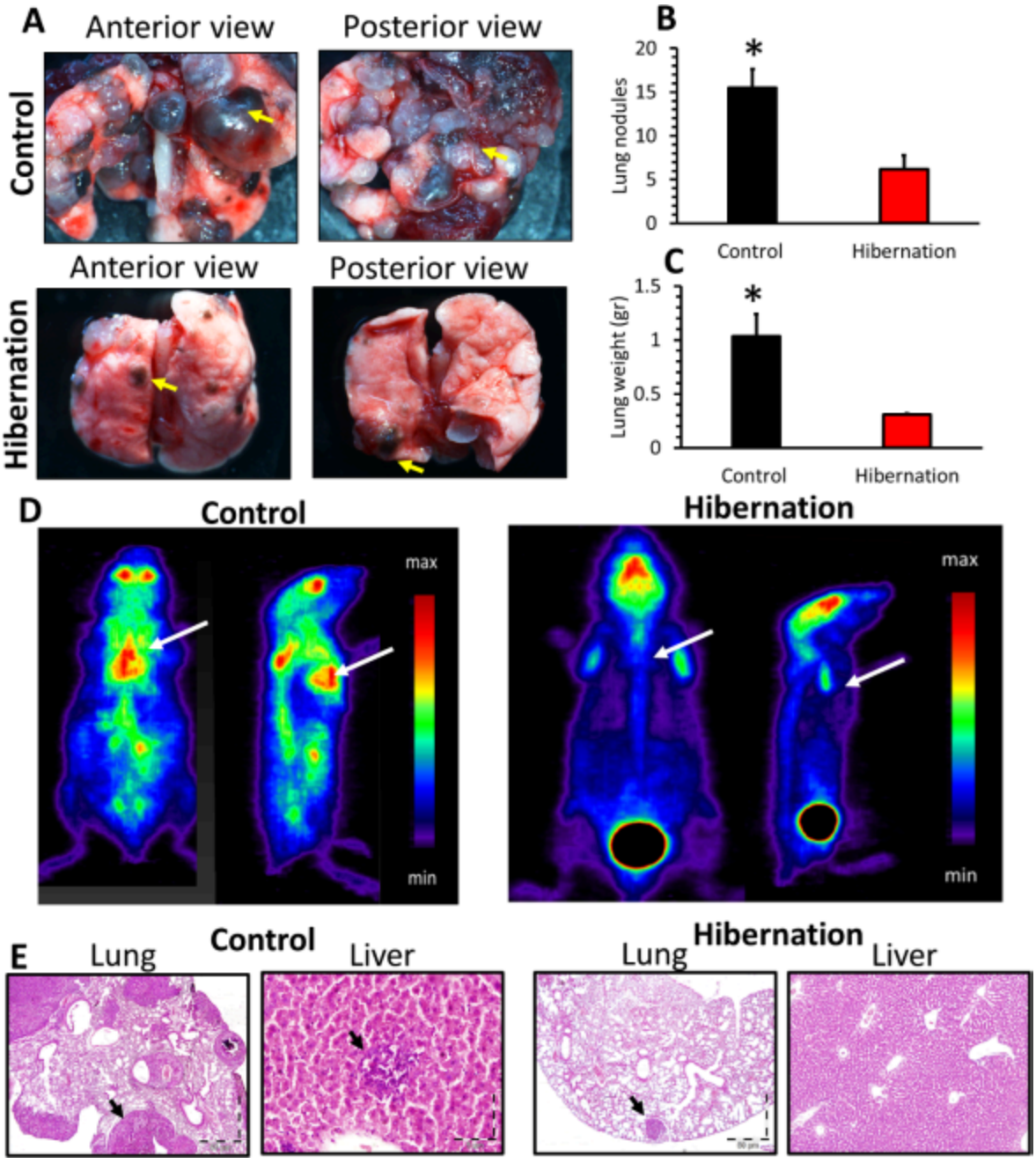


Figure 4

Figure 3. Effect of artificial hibernation on melanoma metastasis in tumor-bearing mice. (A) Representative macroscopic images of lungs showing metastatic colonies 25 days after intravenous injection of B16-F10 melanoma cells, presented in anterior and posterior views. (B) Quantification of the number of metastatic lung nodules in control and hibernation groups. (C) Total lung weight as an indicator of metastatic tumor burden. (D) Representative ^{18}F-FDG PET images of lung metastatic nodules-bearing mice under control conditions and during artificial hibernation, shown in sagittal and frontal views. Arrows indicate the lung region. A marked reduction in whole-body metabolic activity is

observed during hibernation, including reduced uptake in lung regions with metastatic involvement. Please see Figure S2 as animated GIFs. (E) Representative hematoxylin and eosin (H&E)-stained sections of lung and liver tissues from control and hibernation groups. Black arrows indicate metastatic colonies. Data are presented as mean ± SD. Statistical analysis was performed using an unpaired Student's t-test; ns, not significant; P < 0.05 indicates statistical significance.

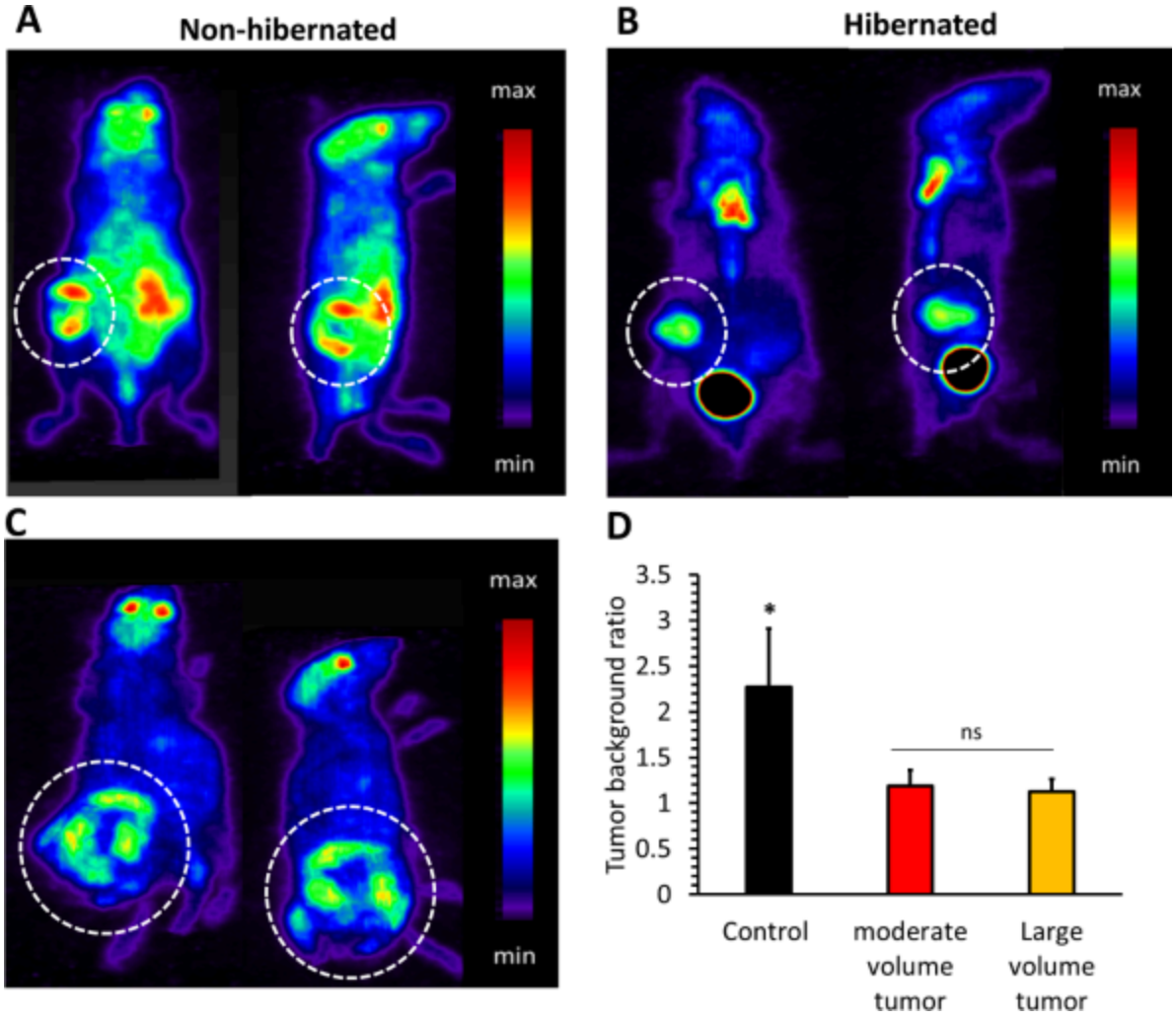


Figure 5

Figure 4. Effect of artificial hibernation on tumor metabolic activity across different tumor sizes. (A) Representative ^{18}F-FDG PET images of non-hibernated control mice. (B) Hibernated mice bearing moderate-volume tumors (14 days post-tumor implantation). (C) Hibernated mice bearing large tumors (28 days post-implantation). Please see Figure S1 as animated GIFs. (D) Quantitative analysis of tumor metabolic activity, expressed as tumor-to-background ratio (TBR), demonstrates a significant reduction in both moderate and large tumors following artificial hibernation in comparison with non-hibernated mice (control). No significant difference in TBR was observed between moderate- and large-tumor groups. Data are presented as mean ± SD. Statistical analysis was performed using an unpaired Student's t-test; ns, not significant; P < 0.05 indicates statistical significance.

Supplementary Files

This is a list of supplementary files associated with this preprint. Click to download.

- Supplement.docx
- clip1.mp4